Inorg. Chem. **2008**, *47*, 1287−1294

Transition Metal Complexes of 3-Cyano- and 3-Nitroformazans

Joe B. Gilroy,[†] Brian O. Patrick,[‡] Robert McDonald,[§] and Robin G. Hicks*[,†]

Department of Chemistry, University of Victoria, P.O. Box 3065, Victoria, BC, Canada V8W 3V6, Crystallography Laboratory, Department of Chemistry, University of British Columbia, Vancouver, BC, Canada V6T 1Z3, and Crystallography Laboratory, Department of Chemistry, University of Alberta, 11227 Saskatchewan Dr. NW, Edmonton, Alberta, Canada T6G 2G2

Received October 8, 2007

The synthesis and characterization of six transition metal complexes of 3-cyano- and 3-nitroformazans are described. Three different formazans were reacted with nickel(II) to produce complexes with bidentate formazan ligands. Mononuclear NiL_2 (L = deprotonated formazan) or binuclear hydroxo-bridged $(LNi)_2(\mu\text{-}OH)_2$ species were produced depending on the steric bulk on the formazan N-aromatic substituents. 1,5-Bis(2-methoxyphenyl)-3-cyanoformazan acts as a tetradentate monoanionic ligand in a copper(II) complex, whereas the analogous 1,5-bis(2-hydroxyphenyl)-3-cyanoformazan binds as a trianion in a tetradentate manner to Fe(III) and Co(III). Crystal structures—the first examples of metal complexes of cyano- or nitroformazans—as well as the electronic spectra of the complexes are discussed in relation to each other as well as that of the uncoordinated formazans.

Introduction

Many of the most popular families of spectator ligands are chelating, anionic, π-conjugated N-donor ligands. Ligands of this general type offer a number of advantages, namely, relatively efficient and versatile synthesis and the ability to control metal complex properties by the choice of substituents at the donor N atoms but also on remote sites (via the π-conjugated framework). Among the many different classes of conjugated polyamido ligands (e.g., amidinates,[1] aminotroponiminates,[2] radical anions of diiminopyridines,[3] and diazabutadienes[4]), in the past decade, the β-diketimines, **1**, have emerged as the most versatile of spectator ligands.[5] The ability to tune steric and electronic properties by modifying R_1 and R_5 (and, to a lesser extent, through changes to R_2, R_3, and R_4) has rendered β-diketimines powerful additions to the stable of benchmark ligand families. The impact of ligand skeleton **1** is further demonstrated through the development of yet more ligand platforms *derived* from β-diketimines, such as the 1,3,5-triazapentadienes (**2**)[6] and the β-ketimines (**3**).[7]

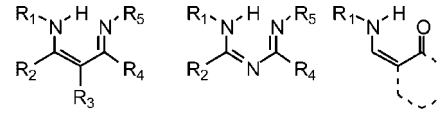

Like the triazapentadienes and β-ketimines, formazans (**4**) are also isostructural to β-diketimines. However, despite the fact that synthetic routes to formazans were well-developed

* Author to whom correspondence should be addressed. E-mail: rhicks@uvic.ca.
† University of Victoria.
‡ University of British Columbia.
§ University of Alberta.

(1) (a) Edelmann, F. T. *Coord. Chem. Rev.* **1994**, *137*, 403. (b) Coles, M. P. *Dalton Trans.* **2006**, 985. (c) Junk, P. C.; Cole, M. L. *Chem. Commun.* **2007**, 1579.
(2) Roesky, P. W. *Chem. Soc. Rev.* **2000**, *29*, 335.
(3) Knijnenburg, Q.; Gambarotta, S.; Budzelaar, P. H. M. *Dalton Trans.* **2006**, 5442.
(4) (a) Gardiner, M. G.; Hanson, G. R.; Henderson, M. J.; Lee, F. C.; Raston, C. L. *Inorg. Chem.* **1994**, *33*, 2456. (b) Scott, P.; Hitchcock, P. B. *J. Chem. Soc., Chem. Commun.* **1995**, 579. (c) Trifonov, A. A.; Fedorova, E. A.; Ikorskii, V. N.; Dechert, S.; Schumann, H.; Bochkarev, M. N. *Eur. J. Inorg. Chem.* **2005**, 2812. (d) Muresan, N.; Chlopek, K.; Weyhermuller, T.; Neese, F.; Wieghardt, K. *Inorg. Chem.* **2007**, *46*, 5327. (e) Trifonov, A. A.; Borovkov, I. A.; Fedorova, E. A.; Fukin, G. K.; Larionova, J.; Druzhkov, N. O.; Cherkasov, V. K. *Chem.—Eur. J.* **2007**, *13*, 4981.
(5) Bourget-Merle, L.; Lappert, M. F.; Severn, J. R. *Chem. Rev.* **2002**, *102*, 3031.
(6) (a) Siedle, A. R.; Webb, R. J.; Behr, F. E.; Newmark, R. A.; Weil, D. A.; Erickson, K.; Naujok, R.; Brostrom, M.; Mueller, M.; Chou, S. H.; Young, V. G., Jr. *Inorg. Chem.* **2003**, *42*, 932. (b) Dias, H. V. R.; Singh, S. *Inorg. Chem.* **2004**, *43*, 5786. (c) Hesse, N.; Frohlich, R.; Humelnicu, L.; Wurthwein, E. U. *Eur. J. Inorg. Chem.* **2005**, 2189. (d) Dias, H. V. R.; Singh, S.; Flores, J. A. *Inorg. Chem.* **2006**, *45*, 8859. (e) Guo, J. P. *Eur. J. Inorg. Chem.* **2006**, 3634. (f) Kopylovich, M. N.; Haukka, M.; Kirillov, A. M.; Kukushkin, V. Y.; Pombeiro, A. I. L. *Chem.—Eur. J.* **2007**, *13*, 786.

10.1021/ic7019846 CCC: $40.75
Published on Web 01/23/2008

over a half-century ago[8] and there are now over *1000* reported derivatives,[9] the coordination chemistry of formazans has not received much attention. We recently described the synthesis and characterization of some boron complexes of 1,3,5-triaryl formazans.[10] Publications describing transition metal−formazan compounds have appeared sporadically since the 1940s.[11–13] There have been almost no systematic investigations,[14] and many of the reported formazan−metal complexes remain inadequately characterized.

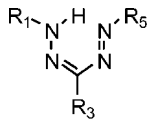

4

The vast majority of β-diketimine complex chemistry has been carried out with ligands with the "nacnac" substitution pattern (**1**; $R_2 = R_4 = Me$; $R_3 = H$). However, there have been reports of complexes of derivatives of **1** containing strong electron-withdrawing groups at R_3, in particular, cyano and nitro groups.[15,16] The strong electron-withdrawing group at R_3 can significantly alter the catalytic activity of resulting complexes.[17] There is little known about any metal complexes of 3-cyano-[18] and 3-nitroformazans[19] beyond their solution spectroscopic properties, although the metal-binding properties of these ligands and associated color changes

Scheme 1

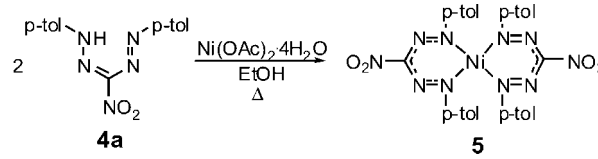

4a **5**

accompanying coordination have led to applications as dyes or as metal-sensing agents.[12,20] We are interested in developing the coordination chemistry of cyano- and nitroformazans, in part because of the novel reactivity of the corresponding β-diketimine complexes and also because we have developed efficient synthetic routes to 3-cyano- and 3-nitroformazans with a range of N-aromatic substituents.[21] Herein, we describe the synthesis and characterization of some first-row transition metal complexes of 3-cyano- and 3-nitroformazans, with a view to establishing the mode of coordination, structures, and spectroscopy of the complexes.

Results and Discussion

Complexes of Bidentate Formazans. The reaction of 1,5-bis(*p*-tolyl)-3-nitroformazan (**4a**) with nickel(II) acetate hydrate produces a discrete Ni(formazan)$_2$ product **5** (Scheme 1). In contrast, the corresponding reaction using the analogous 3-cyanoformazan in place of **4a** yielded completely insoluble and impure materials. The insolubility may be due to the formation of an extended (polymeric) structure in which the cyanoformazan bridges two nickel ions—one via the formazan nitrogen atoms and the other through the cyano substituent.

The ^{1}H and ^{13}C NMR of **5** indicate that all four of the aromatic groups in the complex are equivalent. The X-ray crystal structure of **5** (Figure 1) reveals the structure to consist of two deprotonated formazans chelating to a Ni(II) ion via the substituent-bearing nitrogens. The bond lengths within the formazan ligands (Table 1) indicate that the π system is

(7) (a) Doherty, S.; Errington, R. J.; Housley, N.; Ridland, J.; Clegg, W.; Elsegood, M. R. J. *Organometallics* **1999**, *18*, 1018. (b) Kim, J.; Hwang, J. W.; Kim, Y.; Lee, M. H.; Han, Y.; Do, Y. *J. Organomet. Chem.* **2001**, *620*, 1. (c) Emslie, D. J. H.; Piers, W. E.; MacDonald, R. *J. Chem. Soc., Dalton Trans.* **2002**, 293. (d) Emslie, D. J. H.; Piers, W. E.; Parvez, M.; McDonald, R. *Organometallics* **2002**, *21*, 4226. (e) Emslie, D. J. H.; Piers, W. E.; Parvez, M. *Dalton Trans.* **2003**, 2615. (f) Zhang, D.; Jin, G.; Weng, L.; Wang, F. *Organometallics* **2004**, *23*, 3270. (g) Li, X.; Li, Y.; Li, Y.; Chen, Y.; Hu, N. *Organometallics* **2005**, *24*, 2502. (h) Lyashenko, G.; Saischek, G.; Pal, A.; Herbst-Irmer, R.; Mosch-Zanetti, N. C. *Chem. Commun.* **2007**, 701.

(8) Nineham, A. W. *Chem. Rev.* **1955**, *55*, 355.

(9) Cunningham, C. W.; Burns, G. R.; McKee, V. *J. Chem. Soc., Perkin Trans. 2* **1989**, 1429.

(10) Gilroy, J. B.; Ferguson, M. J.; McDonald, R.; Patrick, B. O.; Hicks, R. G. *Chem. Commun.* **2007**, 126.

(11) (a) Hunter, L.; Roberts, C. B. *J. Chem. Soc.* **1941**, 823. (b) Irving, H.; Gill, J. B.; Cross, W. R. *J. Chem. Soc.* **1960**, 2087. (c) Jameson, G. B.; Muster, A.; Robinson, S. D.; Wingfield, J. N.; Ibers, J. A. *Inorg. Chem.* **1981**, *20*, 2448. (d) Gok, Y.; Senturk, H. B. *Dyes Pigments* **1991**, *15*, 279. (e) Yuzhen, Z.; Dongzhi, L. *Dyes Pigments* **1995**, *29*, 57. (f) Szymczyk, M.; El-Shafei, A.; Freeman, H. S. *Dyes Pigments* **2007**, *72*, 8.

(12) Siedle, A. R.; Pignolet, L. H. *Inorg. Chem.* **1980**, *19*, 2052.

(13) Brown, D. A.; Bogge, H.; Lipunova, G. N.; Muller, A.; Plass, W.; Walsh, K. G. *Inorg. Chim. Acta* **1998**, *280*, 30.

(14) (a) Kawamura, Y.; Ohyanishiguchi, H.; Yamauchi, J.; Deguchi, Y. *Bull. Chem. Soc. Jpn.* **1984**, *57*, 1441. (b) Kawamura, Y.; Deguchi, Y.; Yamauchi, J.; Ohyanishiguchi, H. *Bull. Chem. Soc. Jpn.* **1988**, *61*, 181. (c) Kawamura, Y.; Yamauchi, J.; Ohyanishiguchi, H. *Chem. Lett.* **1990**, 1619. (d) Kawamura, Y.; Yamauchi, J.; Ohyanishiguchi, H. *Bull. Chem. Soc. Jpn.* **1993**, *66*, 3593.

(15) (a) Yokota, S.; Tachi, Y.; Nishiwaki, N.; Ariga, M.; Itoh, S. *Inorg. Chem.* **2001**, *40*, 5316. (b) Allen, S. D.; Moore, D. R.; Lobkovsky, E. B.; Coates, G. W. *J. Organomet. Chem.* **2003**, *683*, 137. (c) Shimokawa, C.; Yokota, S.; Tachi, Y.; Nishiwaki, N.; Ariga, M.; Itoh, S. *Inorg. Chem.* **2003**, *42*, 8395. (d) Shimokawa, C.; Itoh, S. *Inorg. Chem.* **2005**, *44*, 3010. (e) Shimokawa, C.; Tachi, Y.; Nishiwaki, N.; Ariga, M.; Itoh, S. *Bull. Chem. Soc. Jpn.* **2006**, *79*, 118.

(16) Spencer, D. J. E.; Reynolds, A. M.; Holland, P. L.; Jazdzewski, B. A.; Duboc-Toia, C.; Pape, L. L.; Yokota, S.; Tachi, Y.; Itoh, S.; Tolman, W. B. *Inorg. Chem.* **2002**, *41*, 6307.

(17) (a) Allen, S. D.; Moore, D. R.; Lobkovsky, E. B.; Coates, G. W. *J. Am. Chem. Soc.* **2002**, *124*, 14284. (b) Moore, D. R.; Cheng, M.; Lobkovsky, E. B.; Coates, G. W. *Angew. Chem., Int. Ed.* **2002**, *41*, 2599. (c) Moore, D. R.; Cheng, M.; Lobkovsky, E. B.; Coates, G. W. *J. Am. Chem. Soc.* **2003**, *125*, 11911. (d) Byrne, C. M.; Allen, S. D.; Lobkovsky, E. B.; Coates, G. W. *J. Am. Chem. Soc.* **2004**, *126*, 11404. (e) Shimokawa, C.; Teraoka, J.; Tachi, Y.; Itoh, S. *J. Inorg. Biochem.* **2006**, *100*, 1118.

(18) (a) Budesinsky, B. W.; Svec, J. *Inorg. Chem.* **1971**, *10*, 313. (b) Abdelghani, N. T.; Sherif, O. E. *Thermochim. Acta* **1989**, *156*, 69. (c) Sherif, O. E.; Issa, Y. M.; Hassouna, M. E. M.; Abass, S. M. *Monatsh. Chem.* **1993**, *124*, 627. (d) Hassouna, M. E. M.; Issa, Y. M. *J. Indian Chem. Soc.* **1995**, *72*, 709. (e) Darwish, N. A.; AbdelGhani, N. T.; Issa, Y. M.; Tawansi, A.; Sherif, O. E. *J. Indian Chem. Soc.* **1996**, *73*, 103.

(19) (a) Kalia, K. C.; Kumar, A. *Indian J. Chem.* **1978**, *A16*, 52. (b) Kalia, K. C.; Kumar, A.; Singla, M.; Kaur, T. *Indian J. Chem.* **1981**, *A20*, 610. (c) Sharma, R.; Devgan, M.; Kalia, K. C. *Indian J. Chem.* **1996**, *A35*, 63.

(20) (a) Hoshino, H.; Nakano, K.; Yotsuyanagi, T. *J. Chromatogr.* **1990**, *515*, 603. (b) Szymczyk, M.; Czajkowski, W.; Stolarski, R. *Dyes Pigments* **1999**, *42*, 227. (c) Czajkowski, W.; Stolarski, R.; Szymczyk, M.; Wrzeszcz, G. *Dyes Pigments* **2000**, *47*, 143. (d) Ostrovskaya, V. M.; Reshetnyak, E. A.; Nikitina, N. A.; Panteleimonov, A. V.; Kholin, Y. V. *J. Anal. Chem.* **2004**, *59*, 995. (e) Takahashi, T.; Takehara, Y.; Hoshino, H. *Bull. Chem. Soc. Jpn.* **2007**, *80*, 910.

(21) Gilroy, J. B.; Otieno, P. O.; Ferguson, M. J.; McDonald, R.; Hicks, R. G. *Inorg. Chem.* **2008**, *4*, 1279.

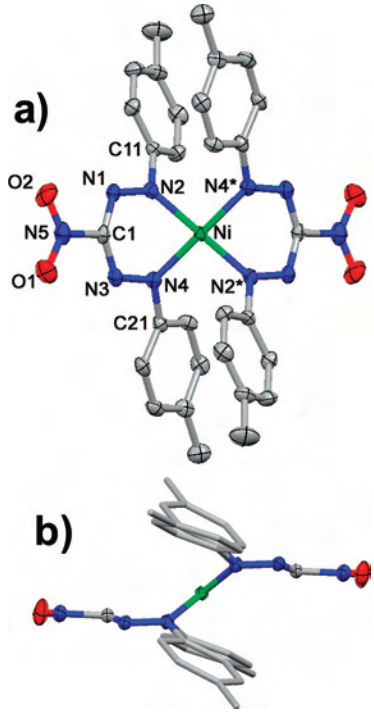

Figure 1. Molecular structure of **5**: (a) top view and (b) side view. Thermal ellipsoids are shown at the 50% probability level. Hydrogen atoms have been removed for clarity.

Table 1. Selected Bond Distances (Å) and Selected Bond Angles (deg) for **5**, **7**, and **8**

	5	7	8
N2−N1	1.293(3)	1.2882(18)	1.288(2)
N3−N4	1.295(3)	1.2860(18)	
N1−C1	1.337(3)	1.332(2)	1.3449(19)
N3−C1	1.330(3)	1.338(2)	
N2−Ni	1.867(2)	1.8304(13)	1.8270(15)
N4−Ni	1.880(2)	1.8305(13)	
Ni−Ni*		2.891	2.898
Ni−O1		1.891(5)	1.854(2)
Ni−O1*		1.884(5)	
N2−N1−C1	116.8(2)	118.36(13)	119.32(17)
N4−N3−C1	116.8(2)	118.22(13)	
N1−N2−Ni	122.97(18)	127.91(11)	128.60
N3−N4−Ni	122.79(18)	128.20(11)	
N2−Ni−N4	85.66(10)	92.54(6)	
Ni−O1−Ni*		100.0(2)	102.81(18)

highly delocalized; within experimental error, there is no bond-length alternation (as suggested by a single canonical resonance structure with alternating single and double bonds). The delocalized structure of coordinated formazans appears to be the norm.[10,12,22] The nickel has a fairly standard square-planar geometry, although the presence of aryl substituents on each of the donor atoms on the two chelating ligands precludes the ligand plane from being coplanar with the nickel square plane. As a result, the nickel ion resides in between the planes defined by N1−N4 of each ligand (Figure 1b); these two planes are 1.67 Å apart, and the nickel ion sits halfway between them (i.e., the nickel atom is 0.83 Å out of the plane of each of the ligands). The nickel square plane (N2, N4, Ni, N2*, N4*) is tilted by 37.3° with respect to the formazan ligand planes, which permits the aromatic

(22) Dale, D. *J. Chem. Soc. A* **1967**, 278.

Scheme 2

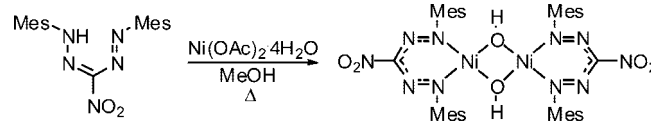

groups to stack over one another in a scissor-type structure. The proximity of the two ligand planes forces the aromatic rings sufficiently close together so that they appear to be repelling one another. These gross structural features are similar to those found in a Pd(II) complex of a 1,3,5-triarylformazan **6**; in this structure, the larger metal forces the two ligand planes even farther apart (2.114 Å) and the Pd square plane is more tilted (43.2°) with respect to the ligand planes.[12]

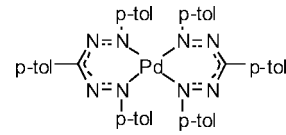

6

A final aspect of the structure of **5** concerns the fact that the meso carbon (C1) is displaced from the N1−N2−N3−N4 plane (by 0.238 Å) in the same face in which the nickel ion is displaced, causing the overall metallacycle ring to appear as a boat conformation. The geometry at C1 is also slightly pyramidalized ($\Sigma\theta$ = 356.7°). Although we do not have an explanation for the unusual structure features associated with C1 in this structure, we do note that these features have been seen in structures of other chelating formazan complexes.[22,23]

The reaction of 1,5-bis(mesityl)-3-nitroformazan **4b** and $Ni(OAc)_2{\cdot}4H_2O$ does not produce a monometallic complex analogous to that obtained using formazan **4a**, presumably because the bulkier mesityl groups in **4b** preclude formation of the bis(chelate) structure observed for **5**. Instead, a bimetallic complex, **7**, containing two (formazan)Ni(II) fragments linked by two bridging hydroxo groups, was obtained (Scheme 2). The bridging hydroxides are confirmed by a strong, sharp alcohol stretch at 3601 cm^{-1} in the infrared spectrum and by a singlet at −6.61 ppm in the ^1H NMR spectrum.[24]

The structure of **7** is shown in Figure 2; the molecule resides on a crystallographic inversion center. The formazan ligand backbone is again delocalized (Table 1) and in addition does not show any of the unusual pyramidalization seen at the C1 carbon in the structure of **5**. The nickel ions are only displaced from the ligand planes by 0.302 Å and are 2.891 Å apart from one another. The Ni_2O_2 core of the structure is planar and diamond-shaped with the nickel ions separated by 2.89 Å. The Ni_2O_2 plane is titled with respect

(23) Polyakova, I. N.; Starikova, Z. A.; Olkhovikova, N. B. *Kristallografiya* **1990**, *35*, 1133.

(24) (a) Lopez, G.; Garcia, G.; Sanchez, G.; Garcia, J.; Ruiz, J.; Hermoso, J. A.; Vegas, A.; Martinezripoll, M. *Inorg. Chem.* **1992**, *31*, 1518. (b) Pickel, M.; Casper, T.; Rahm, A.; Dambouwy, C.; Chen, P. *Helv. Chim. Acta* **2002**, *85*, 4337.

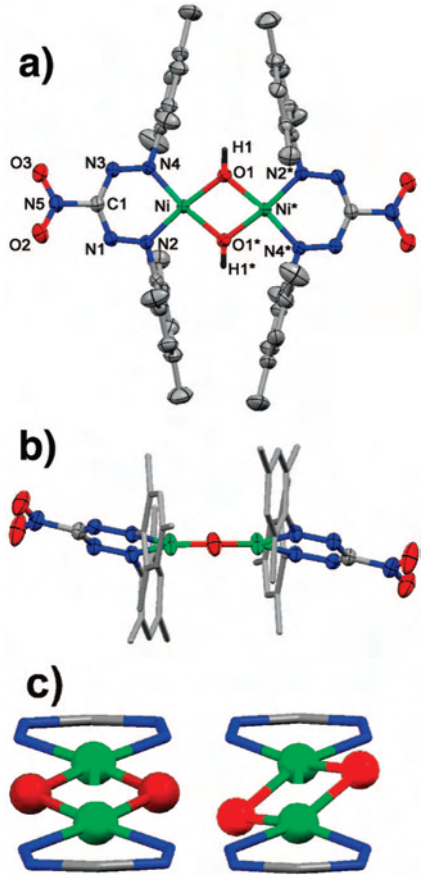

Figure 2. Molecular structure of **7**: (a) top view, (b) side view, and (c) longitudinal view of Ni_2O_2 core showing the two possible positions of the oxygen atoms. Thermal ellipsoids are shown at the 50% probability level. Hydrogen atoms (with the exception of the hydroxyl protons) have been removed for clarity.

Scheme 3

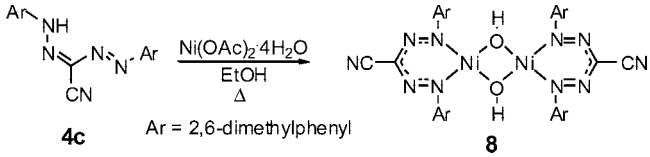

to the formazan backbone plane (N1−N2−C1−N3−N4) both longitudinally (along the long axis of the complex) and laterally; in addition, the oxygen atoms are disordered, leading to two possible relative orientations of the Ni_2O_2 core with respect to the plane of the coordinated formazans (Figure 2c). The N2- and N4-bound mesityl rings have dihedral angles of 77.36° and 83.26°, respectively, with respect to the ligand backbone planes. This aromatic substituent twisting behavior has not been seen before in formazan chemistry, for the simple reason that there were essentially no examples of formazans themselves incorporating *ortho*-substituted aromatic rings prior to our recent publication.[21] This conformational behavior is, however, typical in complexes of β-diketiminates with 2,6-dimethylphenyl substituents.[16,25]

(25) (a) Fekl, U.; Kaminsky, W.; Goldberg, K. I. *J. Am. Chem. Soc.* **2003**, *125*, 15286. (b) MacAdams, L. A.; Buffone, G. P.; Incarvito, C. D.; Rheingold, A. L.; Theopold, K. H. *J. Am. Chem. Soc.* **2005**, *127*, 1082. (c) Hill, M. S.; Hitchcock, P. B.; Pongtavornpinyo, R. *Dalton Trans.* **2007**, 731.

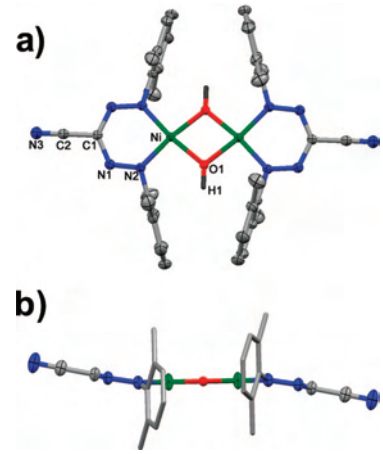

Figure 3. Molecular structure of **8**: top view (a) and side view (b). Thermal ellipsoids are shown at the 50% probability level. Hydrogen atoms (with the exception of the hydroxyl protons) have been removed for clarity.

A hydroxide-bridged binuclear nickel complex, **8**, also resulted from the reaction of 3-cyano-1,5-bis(2,6-methylphenyl)formazan, **4c**, with $Ni(OAc)_2{\cdot}4H_2O$ (Scheme 3). Analogously to **7**, the bridging OH groups give rise to characteristic infrared (ν(OH) 3603 cm^{-1}) and proton NMR spectra (δ(OH) −6.94 ppm). The structure of complex **8** contains bridging oxygens which are disordered in a manner similar to that described for **7**. However, many of the gross structural features described for complex **7** are also seen in **8** (Figure 3), including (i) a delocalized ligand backbone, (ii) nickel ions displaced slightly from the ligand planes (0.211 Å), (iii) an interplanar separation of 0.909 Å between the two formazan ligands, and (iv) aromatic residues that are nearly perpendicular to the formazan backbone plane (85.4°).

From a steric perspective, the structure of **8** is unsurprising because the N-aromatic substituents in **4c** and **4b** both have *ortho*-methyl groups. However, the isostructural nature of **8** and **7** is interesting because the crystal structures (and solution structures) of ligands **4c** and **4b** are different. Nitroformazan **4b** exists exclusively in the *trans-syn*, *s-trans* ("closed") structure depicted in Scheme 2, whereas **4c** is predominantly in the *trans-syn*, *s-trans* ("open") conformation depicted in Scheme 3.[21] Some of the structurally characterized formazan complexes have the formazan ligand chelating to the metal in an asymmetric manner through one divalent nitrogen and one trivalent nitrogen, leading to a five-membered metallacycle ring (**9**) in which the ligand conformation closely resembles an "open" one.[13,28] From this perspective, it is interesting to note that the conformation of the ligand does not necessarily determine the mode of chelation; specifically, ligand **4c**, which is "open", produces a complex in which the formazan has the "closed" structure as a chelate.

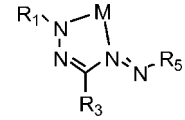

9

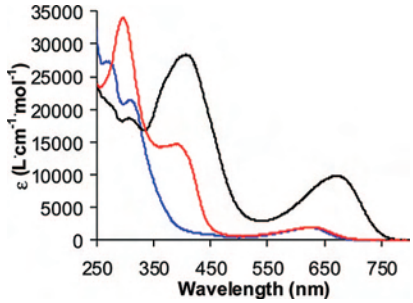

Figure 4. UV–vis spectra of **5** (black line), **7** (red line), and **8** (blue line) in CH_2Cl_2.

Scheme 4

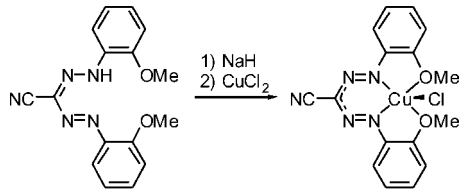

4d **10**

The electronic spectra of complexes **5**, **7**, and **8** are shown in Figure 4. It is well-known that free (noncoordinated) formazans are intensely colored;[8] the absorption wavelength maxima depend on the conformation of the formazan as well as the substitution pattern. Most "closed" formazans have intense ($\epsilon > 10^4$ L cm^{-1} mol^{-1}) absorption maxima between 450 and 550 nm, including **4a** and **4b**;[21] in comparison, the absorption maxima of formazans which adopt the "open structure" are usually blue-shifted (e.g., **4c**, 381 nm).[21] We believe that the lowest energy absorption is therefore charge-transfer in nature involving the N-aromatic substituent and the formazan skeleton. The monometallic bis(formazanato)-Ni(II) **5** has its lowest energy transition maximum at 673 nm. This transition is most likely ligand-based charge transfer (LLCT) and as such is strongly blue-shifted relative to the free ligand **4a** due to a combination of conformational locking of the "closed" ligand structure and enhanced delocalization in the formazan backbone.

The two hydroxo-bridged Ni_2 formazan complexes **7** and **8** have nearly identical low-energy maxima near 620 nm. These maxima are blue-shifted relative to **5** and also have significantly smaller extinction coefficients. We believe that the changes in the spectra of **7** and **8** relative to **5** are related to the structural aspects of the coordinated ligand and *not* to differences in the nature of the complexes (mono vs binuclear). Both **7** and **8** have large torsion angles between the N-aromatic groups and the formazan backbone as a result of steric effects of the *ortho*-methyl substituents. This twisting of N-aromatic groups has been shown to cause both a blue shift and a bleaching effect in the absorption spectra of free formazans,[21] similar to the effects observed for the nickel formazan complexes.

Metal Complexes of Tetradentate Formazans. Additional functional groups (−OH,[26] carboxyl,[27] or N-heterocyclic[13,28]) on the N-aromatic substituents can increase the denticity of formazan ligands. We recently described[21] the synthesis and characterization of bis(*o*-methoxyphenyl) and bis(*o*-hyroxyphenyl) cyanoformazans and present preliminary explorations of their coordination chemistry here. A copper(II) complex, **10**, of 1,5-bis(*o*-methoxyphenyl)-3-cyanoformazan was prepared by the deprotonation of ligand **4d** (sodium hydride) followed by reaction with $CuCl_2$ (Scheme 4). The EPR spectrum of a powder sample of **10** (Figure 5) is typical for a Cu(II) complex, with the unpaired electron occupying the $d_{x^2-y^2}$ orbital.[29] Spectral simulation afforded $g_{\|} = 2.174$, and $g_{\perp} = 2.064$. The room-temperature magnetic moment of **10** is 2.08 μ_B as expected for an $S = {}^1/_2$ Cu(II) ion with $g > 2$.

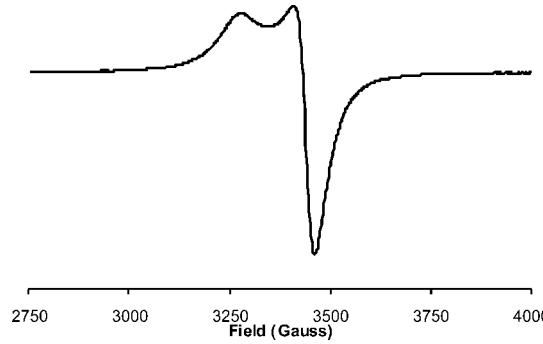

Figure 5. Powder EPR spectrum of **10** at room temperature.

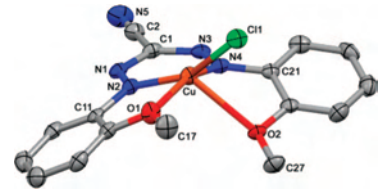

Figure 6. Molecular structure of **10**. Thermal ellipsoids are shown at the 50% probability level. Hydrogen atoms are omitted for clarity.

X-ray-quality crystals of **10** were grown via diffusion of hexanes into a dichloromethane solution. The molecular structure of **10** is shown in Figure 6. The bond lengths within the formazan ligand backbone indicate that it is fully delocalized. The 2-methoxyphenyl substituents are twisted with respect to the formazan plane (N1−N2−C1−N3−N4) by 23.76° (ring attached to N2) and 25.61° (ring attached to N3). The geometry around the copper center is irregular and can be described only as pseudo-five-coordinate; one of the Cu−O bonds is considerably longer (Cu−O2, 2.479(2)Å) than the other (Cu−O1, 2.068(2) Å). The copper atom lies 0.487Å above the plane of the formazan skeleton.

The electronic spectrum of **10** is shown in Figure 7 along with the spectrum of ligand **4d** for comparison. The free ligand has an intense LLCT transition at 464 nm; as was seen for the nickel formazan complexes, coordination causes this transition to be red-shifted (λ_{max} 547 nm) due to the increased delocalization and conformational constraints associated with coordination.

(26) (a) Renkema, W. E.; Lute, C. N.; Stam, C. H. *Acta Crystallogr., Sect. B* **1979**, *35*, 75. (b) Meuldijk, J.; Renkema, W. E.; Vanherk, A. M.; Stam, C. H. *Acta Crystallogr., Sect. C* **1983**, *39*, 1536.
(27) Balt, S.; Klok, C.; Meuldijk, J.; Deboer, J.; Stam, C. H. *Acta Crystallogr., Sect. C* **1985**, *41*, 528.
(28) Takhirov, T. G.; Aleksandrov, Y. I.; Lipunova, G. N.; Rusinova, L. I.; Klyuev, N. A.; Kozina, O. A.; Dyachenko, O. A.; Atovmyan, L. O. *Zh. Obshch. Khim.* **1989**, *59*, 2362.
(29) Garribba, E.; Micera, G. *J. Chem. Educ.* **2006**, *83*, 1229.

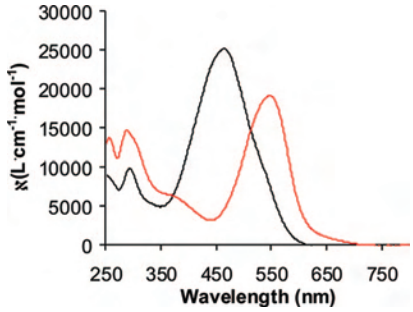

Figure 7. UV–vis spectra of **4d** (black line) and **10** (red line) in CH_2Cl_2.

Scheme 5

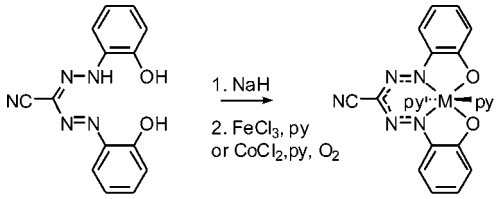

4e

11a M = Fe
11b M = Co

1,5-Bis(2-hydroxyphenyl)-3-cyanoformazan **4e** has also been employed as a ligand. Mononuclear iron and cobalt complexes **11a** and **11b** were prepared by reaction of the deprotonated ligand with $FeCl_3$ or $CoCl_2$ in the presence of pyridine (Scheme 5). In the case of cobalt, air oxidation resulted in isolation of the complex in the Co(III) state. The room-temperature magnetic moment of **11a** is 1.82 μ_B, indicating that the Fe(III) ion is low-spin. The ^{1}H NMR spectrum of **11b** is consistent with two equivalent pyridine ligands and two equivalent *ortho*-substituted aromatic rings.

The structure of **11a** is shown in Figure 8. The iron center is *pseudo*-octahedral; the four equatorial sites are occupied by the delocalized and completely planar (including the *ortho*-phenyl substituents) tetradentate formazan ligand, while two pyridine ligands coordinate to the two axial positions. The iron center lies in the same plane as the formazan. Each of the coordinated pyridines is oriented such that their ring planes bisect the N2−Fe−N4 bond angle (i.e., they are essentially coincident with the axis defined by the cyano substituent, Figure 8b). The corresponding Co(III) complex, **11b**, is isostructural to **11a** and as such shares all of the qualitative structural features described above; pertinent bond lengths and angles for these two structures are summarized in Table 2.

The electronic spectra of complexes **11a** and **11b** and free formazan **4e** are presented in Figure 9. As previously discussed,[21] the uncoordinated ligand has an intense absorption maximum at 480 nm, and another transition is also apparent on the low-energy shoulder of this absorption peak. The 480 nm peak appears to remain unchanged in the spectra of the two complexes **11a** and **11b**, but the extinction coefficients of this peak are much smaller in the complexes. The spectra of the complexes have additional absorption peaks in the UV (λ_{max} = 322 nm for **11a** and λ_{max} = 325 nm for **11b**) and in the visible (λ_{max} = 592 and 631 nm for **11a** and λ_{max} = 608 and 658 nm for **11b**) spectra. The qualitative similarities between the spectra of **11a** and **11b** suggest that these transitions are ligand-based in character, although the possibility that some of them may be charge-transfer bands (ligand-to-metal or metal-to-ligand charge transfer) cannot be excluded.

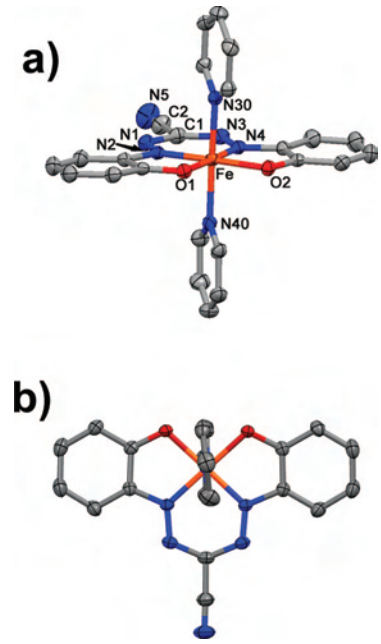

Figure 8. Molecular structure of **11a**: (a) partial atom labeling scheme and (b) view down the N30−Fe−N40 axis. Thermal ellipsoids are shown at the 50% probability level. Hydrogen atoms are removed for clarity.

Table 2. Selected Bond Distances (Å) and Selected Bond Angles (deg) for **9**, **11a**, and **11b**

	10 (M = Cu)	**11a** (M = Fe)	**11b** (M = Co)
N2−N1	1.297(4)	1.310(3)	1.288(3)
N3−N4	1.286(4)	1.310(3)	1.286(3)
N1−C1	1.340(5)	1.352(4)	1.357(4)
N3−C1	1.354(5)	1.347(4)	1.358(4)
N2−M	1.928(3)	1.846(2)	1.856(2)
N4−M	1.946(3)	1.849(2)	1.860(2)
M−O1	2.068(3)	1.9121(17)	1.8979(17)
M−O2	2.479(2)	1.9218(18)	1.9075(18)
M−Cl1	2.2147(10)		
M−N30		2.010(2)	1.966(2)
M−N40		1.997(2)	1.954(2)
N2−N1−C1	118.9(3)	117.6(2)	117.5(2)
N4−N3−C1	118.5(3)	118.0(2)	117.8(2)
N1−N2−M	127.8(3)	128.83(17)	128.17(17)
N3−N4−M	127.8(3)	128.45(18)	127.79(19)
N2−M−O1	80.10(12)	86.29(8)	86.42(9)
N4−M−O2	71.26(10)	86.08(8)	85.97(9)
N2−M−N4	87.62(13)	93.49(9)	94.22(10)
O2−M−O1	97.47(9)	94.17(7)	93.41(8)
N2−M−Cl1	155.37(9)		
N4−M−Cl1	103.61(10)		
N30−M−N40		175.96(8)	177.26(8)

Conclusions

We have described preliminary studies of the coordination chemistry of 3-cyano- and 3-nitroformazan ligands. Previously described complexes of these ligands have not been well characterized, particularly with respect to structural data, as there were no structurally characterized cyano- or nitroformazan complexes prior to this work. For all of the complexes discussed herein, the formazans bind to the metal ion via the N1 and N5 atoms to produce a six-membered metallacycle; no five-

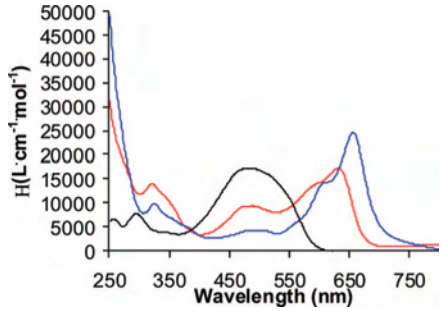

Figure 9. UV–vis spectra of **4e** (black line), **11a** (red line), and **11b** (blue line) in CH_2Cl_2.

membered metallaformazan rings (**9**) were observed. This is of particular interest with respect to formazan **4c**. Even though it exists as an "open" conformation, which would seem to favor complex structures analogous to **9**, the six-membered chelate ring is formed. This may in part be due to the particular set of substituents in these ligands. The strong electron-withdrawing nature of groups at the C3 position may reduce the coordinating ability of the N2 and N4 atoms through a combination of inductive and resonance effects. In a more general context, this suggests that, although isomerism is a common facet of formazans, the particular structure adopted by a given formazan may not have direct implications for its mode of coordination; the electronic effects of substituents or the presence of additional donor sites (cf. **4d** and **4e**) play a more central role in determining complex structure.

The formazan complexes retain the color characteristics of free ligands, and in this respect, these ligands are distinct from the many other benchmark ancillary ligands. However, aside from this aspect of their chemistry, it remains to be seen whether formazan ligands are merely "nacnac" mimics or whether they convey *other* distinctive properties to the resulting complexes. A particular avenue of interest to us concerns the possibility of alternative electronic structure formulations to the generic one represented by canonical structure **12**. We have already demonstrated that reduction of boron−formazan complexes (**12**; E = $B(OAc)_2$) leads to radical anions **13** (E = $B(OAc)_2$) in which the unpaired electron resides on the formazan ligand, thus justifying its description as a "borataverdazyl".[10] The formazan complexes described herein are clear examples of the general structure **12** where E is a transition metal fragment; attempts to realize "metalloverdazyl"-type systems, **13**, are in progress and will be reported in due course.

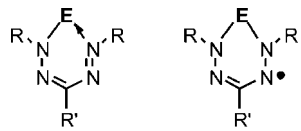

12 **13**

Experimental Section

General Considerations. All reactions and manipulations were carried out under an argon atmosphere using standard Schlenk or glovebox techniques unless stated otherwise. Solvents were dried and distilled under argon prior to use. All reagents were purchased from Aldrich and used as received. The synthesis of formazans **4a**−**e** have been described.[21] NMR spectra were recorded on a 300 MHz Bruker instrument. EPR spectra were recorded on a Bruker EMX EPR instrument equipped with an X-band microwave bridge. Infrared spectra were recorded as KBr pellets using a Perkin-Elmer Spectrum One instrument. UV–vis spectra were recorded using a Cary 50 Scan instrument. Elemental analyses were carried out by Canadian Microanalytical Services Ltd., Vancouver, BC.

X-Ray Structure Determinations. X-ray diffraction data were collected on a Bruker PLATFORM/SMART 1000 CCD with graphite-monochromatized Mo Kα radiation ($\lambda = 0.71073$ Å). The crystal structures were solved by direct methods (SHELXS-97); see Table 3 for crystallographic data.

Synthesis of Bis(3-nitro-1,5-*p*-tolylformazanato)nickel (5). Formazan **4a** (0.400 g, 1.3 mmol), nickel acetate tetrahydrate (0.167 g, 0.67 mmol), and 95% ethanol (50 mL) were combined and allowed to reflux open to the air for 16 h. After cooling to room temperature, the mixture was filtered and the solid washed with 95% ethanol (3 × 10 mL), affording **5** as a dark green microcrystalline solid, yield: 0.362 g (85.5%). X-ray-quality crystals were grown via diffusion of pentane into a solution of **5** in dichloromethane. Mp.: 358–360 °C. ^{1}H NMR (CD_2Cl_2): δ 7.42 (d, 4H, ^3J = 8 Hz), 7.00 (d, 4H, ^3J = 8 Hz), 2.34 (s, 6H). ^{13}C NMR (CD_2Cl_2): δ 148.7, 140.5, 129.9, 123.6, 21.5 ppm. FT-IR (KBr): 1525 (m), 1355 (s), 1275 (s), 819 (m) cm^{-1}. UV–vis (CH_2Cl_2): λ_{max} 310 nm (ϵ = 18 500), 409 nm (ϵ = 27 500), 673 nm (ϵ = 10 000). Anal. calcd for $NiC_{30}H_{28}N_{10}O_4$: C, 55.32; H, 4.33; N, 21.51. Found: C, 55.06; H, 4.22; N, 20.97.

Synthesis of Bis-(1,5-mesityl-3-nitroformazanato)-bis-μ-hydroxonickel (7). Formazan **4b** (0.610 g, 1.7 mmol), nickel acetate tetrahydrate (0.430 g, 1.7 mmol), and methanol (100 mL) were combined and allowed to reflux open to the air for 16 h. After cooling to room temperature, the mixture was filtered and the solid washed with methanol (3 × 10 mL), affording **7** as a dark green microcrystalline solid, yield: 0.431 g (59.2%). X-ray-quality crystals were grown via vapor diffusion of pentane into a solution of **7** in dichloromethane. Mp.: 276–278 °C (dec). ^{1}H NMR (CD_2Cl_2): δ 6.61 (s, 8H), 2.41 (s, 24H), 2.26 (s, 12H), −6.61 (s, 2H, μ-OH). ^{13}C NMR (CD_2Cl_2): δ 143.1, 138.4, 130.8, 129.6, 21.5, 18.5 ppm. FT-IR (KBr): 3601 (m) (OH), 1537 (s), 1371 (s), 1355 (s), 1294 (s), 761 (s) cm^{-1}. UV–vis (CH_2Cl_2): λ_{max} 298 nm (ϵ = 34 000), 392 nm (ϵ = 14 750), 635 nm (ϵ = 2000). Anal. calcd for $Ni_2C_{38}H_{46}N_{10}O_2$: C, 53.30; H, 5.42; N, 16.36. Found: C, 53.30; H, 5.48; N, 16.45.

Synthesis of Bis-(3-cyano-1,5-(2,6-dimethylphenyl)formazanato)-bis-μ-hydroxonickel (8). Formazan **4c** (0.540 g, 1.8 mmol), nickel acetate tetrahydrate (0.440 g, 1.8 mmol), and 95% ethanol (100 mL) were combined and allowed to reflux open to the air for 16 h. After cooling to room temperature, the mixture was filtered and the solid washed with 95% ethanol (3 × 10 mL), affording **8** as a dark green microcrystalline solid, yield: 0.440 g (32.2%). X-ray-quality crystals were grown via diffusion of pentane into a solution of **8** in dichloromethane. Mp.: 266–268 °C (dec). ^{1}H NMR (CD_2Cl_2): δ 6.87 (t, 4H, ^3J = 7 Hz), 6.73 (d, 8H, ^3J = 8 Hz), 2.41 (s, 24H), −6.94 (s, 2H, μ-OH). ^{13}C NMR (CD_2Cl_2): δ 145.2, 130.9, 129.2, 129.1, 18.3 ppm. FT-IR (KBr): 3603 (m) (OH), 2229 (m) (CN), 1358 (s) cm^{-1}. UV–vis (CH_2Cl_2): λ_{max} 271 nm (ϵ = 27 500), 307 nm (ϵ = 21 500), 620 nm (ϵ = 1950). Anal. calcd for $Ni_2C_{36}H_{38}N_{10}O_2$: C, 56.88; H, 5.04; N, 18.43. Found: C, 56.99; H, 5.13; N, 18.32.

Copper(3-cyano-1,5-(2-methoxyphenylformazanato)chloride (10). Formazan **4d** (1.00 g, 3.2 mmol) was combined with freshly distilled tetrahydrofuran (100 mL) under argon and treated with sodium hydride (0.080 g, 3.3 mmol) before it was allowed to stir for 16 h, changing in color from red to brown-red. Copper(II) chloride (0.432 g, 3.3 mmol) was added, and the reaction was once again left to stir for 16 h. The solvent was then removed and the

Table 3. Crystallographic Data

compound	**5**	**7**	**8**	**9**	**10a**	**10b**
formula	$C_{30}H_{28}N_{10}O_4Ni$	$C_{38}H_{46}N_{10}Ni_2O_6{\bullet}0.5C_5H_{12}$	$C_{36}H_{38}N_{10}O_2Ni_2{\bullet}1.25CH_2Cl_2$	$C_{16}H_{14}N_5O_2CuCl$	$C_{24}H_{18}N_7O_2Fe{\bullet}CH_2Cl_2$	$C_{24}H_{18}N_7O_2Co{\bullet}CH_2Cl_2$
fw	651.33	892.34	866.34	407.31	577.23	580.31
dimensions (mm)	0.05 × 0.12 × 0.30	0.54 × 0.41 × 0.17	0.15 × 0.25 × 0.50	0.02 × 0.05 × 0.50	0.38 × 0.34 × 0.23	0.66 × 0.42 × 0.33
a (Å)	12.5875(13)	11.6602 (14)	15.3752(8)	13.328(2)	9.0144(6)	8.9601 (8)
b (Å)	7.4705(9)	19.801 (2)	16.4725(8)	7.1885(6)	9.3053(6)	9.3250 (8)
c (Å)	16.707(2)	19.807 (2)	10.6976(5)	17.422(2)	15.8871(11)	15.8258 (13)
cryst syst	monoclinic	monoclinic	monoclinic	monoclinic	triclinic	triclinic
α (deg)	90	90	90	90	73.7154 (8)	73.4386 (10)
β (deg)	103.689(4)	92.5918 (16)	132.934(2)	91.044(3)	87.5893 (9)	87.6027 (10)
γ (deg)	90	90	90	90	87.5292 (9)	87.5323 (11)
volume (Å^3)	1526.4(3)	4568.5 (9)	1983.6(2)	1668.8(3)	1277.36 (15)	1265.66 (19)
space group	$P2_1/c$ (#14)	*C*2/*c* (#15)	*C*2/*m* (#12)	$P2_1/n$ (#14)	*P* (#2)	*P* (#2)
Z	2	4	2	4	2	2
μ (mm^{-1})	0.689	0.878	1.164	1.489	0.837	0.927
T (K)	193.15	193.15	193.15	193.15	193.15	193.15
independent reflections	2692, R_{int} = 0.073	5301, R_{int} = 0.0300	2444, R_{int} = 0.028	2942, R_{int} = 0. 074	5180, R_{int} = 0.0178	5083, R_{int} = 0.0119
R	0.041	0.0372	0.042	0.073	0.0492	0.0496
wR	0.071	0.1035	0.101	0.088	0.1510	0.1468

solid triturated with hexanes (100 mL). The solid was then dissolved in dichloromethane (3 × 150 mL), leaving behind a small amount of brown solid byproduct. The solution was filtered before being concentrated in vacuo, affording **10** as a dark purple solid (green reflex), yield: 1.00 g (75.9%). X-ray-quality crystals were grown from the solvent diffusion of hexanes into a dichloromethane solution of **10**. Mp.: 180–182 °C (dec., brown). FT-IR (KBr): 2225 (m) (CN), 1587 (m), 1483 (m), 1344 (s), 752 (s) cm^{-1}. UV–vis (CH_2Cl_2): λ_{max} 256 nm (ϵ = 13 750), 288 nm (ϵ = 14 750), 371 nm (ϵ = 6250), 547 nm (ϵ = 19 250). Anal. calcd for $C_{19}H_{16}N_4$: C, 47.18; H, 3.46; N, 17.19. Found: C, 47.21; H, 3.81; N, 16.87.

Iron(3-cyano-1,5-(2-hydroxyphenylformazanato)-bis-pyridine (11a). Formazan **4e** (0.250 g, 0.88 mmol) was combined with freshly distilled tetrahydrofuran (100 mL) under argon and treated with sodium hydride (0.064 g, 2.7 mmol) before being left to stir for 16 h, changing in color from red to dark blue. Iron(III) chloride (0.144 g, 0.88 mmol) and pyridine (0.36 mL, 4.5 mmol) were added, and the reaction was left to stir for 16 h, at which time the solution was a dark blue color. The mixture was then filtered, and the solvent was removed *in vacuo*. Trituration with hexanes allowed for **11a** to be isolated as a dark blue solid (bronze reflex), yield: 0.317 g (72.9%). X-ray-quality crystals were grown from the solvent diffusion of hexanes into a dichloromethane solution of **11a**. Mp.: 270–272 °C. FT-IR (KBr): 2225 (m) (CN), 1577 (m), 1459 (s), 1448 (s), 1300 (s) cm^{-1}. UV–vis (CH_2Cl_2): λ_{max} 234 nm (ϵ = 32 500), 320 nm (ϵ = 14 000), 484 nm (ϵ = 9250), 592 nm (ϵ = 13 750), 631 nm (ϵ = 17 250). Anal. calcd for $FeC_{24}H_{18}N_7O_2$: C, 58.55; H, 3.69; N, 19.92. Found: C, 57.63; H, 3.82; N, 19.36.

Cobalt(3-cyano-1,5-(2-hydroxyphenylformazanato)-bis-pyridine (11b). Formazan **4e** (0.250 g, 0.88 mmol) was combined with freshly distilled tetrahydrofuran (100 mL) under argon and treated with sodium hydride (0.064 g, 2.7 mmol) before being left to stir for 16 h, changing in color from red to dark blue. Cobalt(II) chloride (0.115 g, 0.88 mmol) and pyridine (0.36 mL, 4.5 mmol) were added, and the reaction was left to stir for 16 h, at which time the solution had changed to a red-brown color. The mixture was then allowed to stir open to the air, changing in color to dark blue before the solution was filtered and the solvent removed *in vacuo*. Trituration with hexanes allowed **11b** to be isolated as a dark blue solid (bronze reflex), yield: 0.325 g (74.3%). X-ray-quality crystals were grown from the solvent diffusion of hexanes into a dichloromethane solution of **11b**. Mp.: 262–264 °C. ^{1}H NMR (CD_2Cl_2): δ 7.99 (d of d, 2H, ^3J = 7 Hz, ^4J = 1 Hz), 7.41 (t, 2H, ^3J = 7 Hz), 7.37 (d, 4H, ^3J = 7 Hz), 7.14 (d of d, 2H, ^3J = 8 Hz, ^4J = 1 Hz), 6.98 (t of d, 2H, ^3J = 7 Hz, ^4J = 1 Hz), 6.91 (t, 4H, ^3J = 7 Hz), 6.53 (t of d, 2H, ^3J = 7 Hz, ^4J = 1 Hz). ^{13}C NMR (CD_2Cl_2): δ 168.4, 151.6, 147.5, 139.2, 130.4, 125.1, 119.4, 116.4, 116.2 ppm. FT-IR (KBr): 2219 (m) (CN), 1462 (s), 1448 (s), 1234 (s) cm^{-1}. UV–vis (CH_2Cl_2): λ_{max} 242 nm (ϵ = 42 500), 325 nm (ϵ = 10 000), 483 nm (ϵ = 4250), 509 nm (ϵ = 4250), 608 nm (ϵ = 14 500), 658 nm (ϵ = 24 750). Anal. calcd for $CoC_{24}H_{18}N_7O_2$: C, 58.19; H, 3.66; N, 19.79. Found: C, 57.78; H, 3.79; N, 19.39.

Acknowledgment. Financial support from the University of Victoria, The Natural Sciences and Engineering Research Council of Canada, and the Petroleum Research Fund of the American Chemical Society is gratefully acknowledged.

Supporting Information Available: Characterization and crystallographic information for compounds **5**, **7**, **8**, **10**, **11a**, and **11b**. This material is available free of charge via the Internet at http://pubs.acs.org.

IC7019846